Journal of Alloys and Compounds 857 (2021) 157587

Contents lists available at ScienceDirect

Journal of Alloys and Compounds

journal homepage: http://www.elsevier.com/locate/jalcom

New evidences for understanding the serrated flow and shear band behavior in nanoindentation of metallic glasses

Hu Huang [a, b, *], Minqiang Jiang [c, d], Jiwang Yan [b]

[a] Key Laboratory of CNC Equipment Reliability, Ministry of Education, School of Mechanical and Aerospace Engineering, Jilin University, Changchun, Jilin, 130022, China
[b] Department of Mechanical Engineering, Faculty of Science and Technology, Keio University, Yokohama, 223-8522, Japan
[c] State Key Laboratory of Nonlinear Mechanics, Institute of Mechanics, Chinese Academy of Sciences, Beijing, 100190, People's Republic of China
[d] School of Engineering Science, University of Chinese Academy of Sciences, Beijing, 100049, PR China

ARTICLE INFO

Article history:
Received 9 December 2019
Received in revised form
4 October 2020
Accepted 13 October 2020
Available online 14 October 2020

Keywords:
Nanoindentation
Bulk metallic glass
Shear band
Serrated flow

ABSTRACT

Nanoindentation of a Zr-based metallic glass was performed under various loading rates by using a cube-corner indenter. Experimental results showed that increasing the loading rate from 2 to 20 mN/s, the size of serrated flow was greatly weakened, but the number of serrated flow kept very stable, together with very similar shear band features around the residual indents. These results challenge the current understanding derived from the results obtained by using the Berkovich indenter, and can be well explained by the shear-band propagation dynamics model, i.e., loading rate impeded the propagation of shear band rather than its nucleation.

1. Introduction

Metallic glasses (MGs) are quite promising materials due to their unique mechanical, physical, and chemical properties [1–3]. However, the very limited plasticity in tension significantly impedes their practical applications as structural and engineering materials. Therefore, further improving the plasticity of MGs is quite important [1,4–7], for which the first step is to completely understand its plastic deformation mechanism. For this purpose, large amounts of efforts have been attempted and significant progress has been achieved [8–13]. Currently, a common view is reached that shear banding is the main plastic deformation mechanism for MGs [14,15], but it is not easy to directly investigate the shear banding because of absence of suitable characterization techniques [16]. Alternatively, the serrated flow phenomenon observed in the stress-strain curve in tension or compression testing as well as load-depth curve in nanoindentation testing of MGs [17–23], opens a window for indirectly studying the shear banding because serrated flow is regarded as the consequence of operation of shear band such as nucleation, propagation, intersection, and arrest. Previous studies [24–32] indicated that serrated flow is sensitive to the strain rate; when the strain rate increases from the low one to the high one, the transition from serrated to non-serrated flow occurs. To explain this transition, currently, two models are widely employed, shear-band nucleation dynamics (SBND) model [17,18,33] and shear-band propagation dynamics (SBPD) model [16,25], which are derived from the results of nanoindentation and compression testing, respectively. The former one argues that high strain rate stimulates high nucleation rate of shear band, and the latter one argues that the transition is directly linked to the propagation velocity of shear band. Although both of these two models could explain some specific phenomena, further investigation should be conducted for achieving a general model. Moreover, being different from the common view that promoted serrated flows correspond to increased shear bands, some opposite results are recently reported that prompted serrated flows correspond to few surface shear bands [34,35]. For example, nanoindentation results of pre-compressed $Zr_{65}Cu_{15}Al_{10}Ni_{10}$ MGs showed that under specific pre-compression deformation, the indentation curve presented increased serrated flows but the corresponding residual indent showed less surface shear bands [34].

* Corresponding author. Key Laboratory of CNC Equipment Reliability, Ministry of Education, School of Mechanical and Aerospace Engineering, Jilin University, Changchun, Jilin, 130022, China.
E-mail address: huanghu@jlu.edu.cn (H. Huang).

https://doi.org/10.1016/j.jallcom.2020.157587
0925-8388/

Similar results were also observed for the nanosecond pulsed laser irradiated surface of a Zr-based MG [35]. These phenomena challenge the current understanding of the correlation between the serrated flow and shear band behavior.

In this study, to further understand the serrated flow and shear band behavior, a cube-corner indenter was employed to characterize the nanoindentation response of a $Zr_{41.2}Ti_{13.8}Cu_{12.5}Ni_{10}Be_{22.5}$ MG. The cube-corner indenter has a same shape with that of the commonly used Berkovich indenter, i.e., the pyramidal shape, but the face angle of the cube-corner indenter (35.26°) is much smaller than that of the Berkovich indenter (65.27°) [36]. That is to say, the cube-corner indenter is much sharper compared to the Berkovich indenter, and thus it could produce much higher contact stress and strain [37]. Therefore, more prominent surface shear bands and serrated flows could be induced by the cube-corner indenter, being beneficial to investigate their correlation. Accordingly, new evidences for further understanding the serrated flow and shear band behavior in nanoindentation of MGs were obtained by comparatively analyzing the serrated flow and shear band under various loading rates.

2. Materials and experiments

The Zr-based MG sample with a thickness of 1 mm and diameter of 10 mm was prepared by wire electrical discharge machining (wire-EDM) of an as-cast MG rod, followed by grinding and polishing using 400, 800, and 1500 grit sand papers and diamond abrasive paste in sequence to remove the crystalline layers generated during EDM [38,39]. Nanoindentation tests were performed by using an ENT-1100 nanoindentation instrument (Elionix Inc., Japan) under the load control mode. For ease of comparison, a consistent indentation load of 100 mN was selected with various loading rates, 2, 10, and 20 mN/s, and the incremental load for adjacent sampling point was kept the same of 0.1 mN. For each condition, eight nanoindentation tests were conducted. A field emission scanning electron microscope (FE-SEM) (JSM-7600F, JEOL, Japan) were used to observe the residual indents.

3. Results and discussion

Fig. 1 shows two representative results obtained under the loading rate of 2 mN/s. Although the experimental conditions are exactly the same, the differences in both shear band and serrated flow are observed. More conspicuous shear bands appear around the residual indent obtained by Test 2 especially in the region circled by dotted-line. Correspondingly, enhanced serrated flows are observed in the load-depth curve of Test 2. This difference is further confirmed by analyzing the depth difference-loading time curves obtained by the depth-difference method [40], where 13 sharp peaks with depth difference being over 20 nm appear for Test 2 but only 5 peaks are over 20 nm for Test 1. These differences in shear band and serrated flow reflect that local inhomogeneity exists in the MG. The comparative results in Fig. 1(a)–(c) confirm the law that for the as-cast MG, the more the shear bands are, the more intense serrated flows will appear. Apart from the remarkable difference in height of the peaks in Fig. 1(c), it is interesting to find that the number of peaks in the time range of 10~50 s (20~100 mN) is almost the same for Test 1 and 2, 25 and 24, respectively. Accordingly, from Fig. 1, it could roughly deduce that the nucleation of shear bands may be the same but their propagation is different,

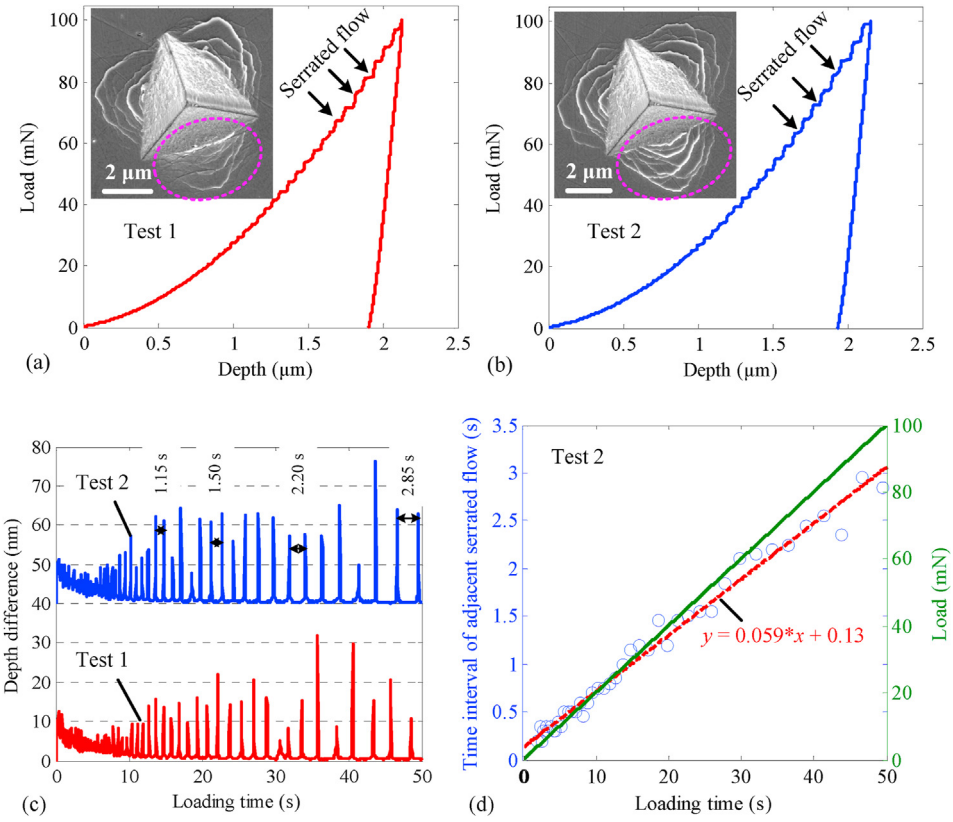

Fig. 1. Results obtained under the loading rate of 2 mN/s. (a) and (b) show the load-depth curves and corresponding morphologies of residual indents. (c) The depth difference varies with the loading time. For ease of comparison, the depth difference of Test 2 is shifted by 40 nm along the vertical axis. (d) Time interval of adjacent serrated flow as well as load varies with the loading time.

resulting in the different height of peaks but almost the same number. Moreover, by recording the time interval of adjacent serrated flow as shown in Fig. 1(c), its correlation with the loading time as well as the indentation load is illustrated in Fig. 1(d). It shows that the time interval tends to linearly increase with increase in the loading time (i.e. the load). By linear fitting, the slope of the fitted line is 0.059.

To further investigate the effects of loading rate on the shear band and serrated flow behavior, Figs. 2 and 3 present the corresponding results obtained under the loading rates of 10 and 20 mN/s, respectively. By comparing the morphologies of residual indents shown in Figs. 1(b), 2(a) and 3(a), it is noted that although the loading rate is quite different, the shear bands generated by the cube-corner indenter show nearly the same features in the aspect of space distribution, shape as well as density.

On the contrary, in both the load-depth curves and depth difference-loading time curves, the serrated flows are remarkably weakened with increase in the loading rate. For example, 24 peaks are over 20 nm for Test 2 in Fig. 1(c) (2 mN/s), only 2 peaks are over 9 nm in Fig. 2(b) (10 mN/s), and all peaks are less than 8 nm when the loading rate is 20 mN/s (not shown here). Although the height of peaks is greatly suppressed in Fig. 2(b), the number of peaks in the time range of 2~10 s (20~100 mN) is 25, being surprisingly very close to that for Test 2. By fitting the time interval-loading time curve, it is found that the slope is 0.054, being very close to that (0.059) for Test 2. This suggests that when the loading rate is increased from 2 to 10 mN, the corresponding time interval of adjacent serrated flow also becomes 5 times. This conclusion can be further confirmed by the correlation curve of time interval in Fig. 2(d) obtained under 2 and 10 mN/s whose slope is 5.5. The small deviation between the measured slope (5.5) and the ideal one (5) may be due to that the corresponding load value of each serrated flow under these two loading rates is not exactly the same. In Fig. 3(b), the slope of the time interval-loading time curve is 0.054 when the loading rate is increased to 20 mN/s, which further confirms that increasing the loading rate, the time interval of adjacent serrated flow is multiplied.

Fig. 4 presents the statistical results of the number of serrated flow in the load range of 20~100 mN under various loading rates. It is noted that although the loading rate is increased from 2 to 20 mN/s, the number of serrated flow in the evaluated load range is in the range of 24~26, being independent of the loading rate.

From Figs. 1–4, the following facts can be obtained. With increase in the loading rate from 2 to 20 mN/s, (1) the shear bands generated around the residual indents show very similar features; (2) the time interval of adjacent serrated flow is multiplied but the slope of the time interval-loading time curve keeps stable; (3) the height of peaks in depth difference-loading time curves is decreased but the number of peaks in the load range of 20~100 mN keeps very stable. These facts challenge our currently understanding that shear bands and serrated flows are very sensitive to the loading rate, and high loading rate greatly suppresses the generation of shear bands and serrated flows, which is mainly derived from the results obtained by using the Berkovich indenter [41]. Compared to the cube-corner indenter, Berkovich indenter is relatively blunted and very few shear bands could be induced around the residual indent [37]. Therefore, the derived conclusion should be not very accurate and sometimes may be questionable.

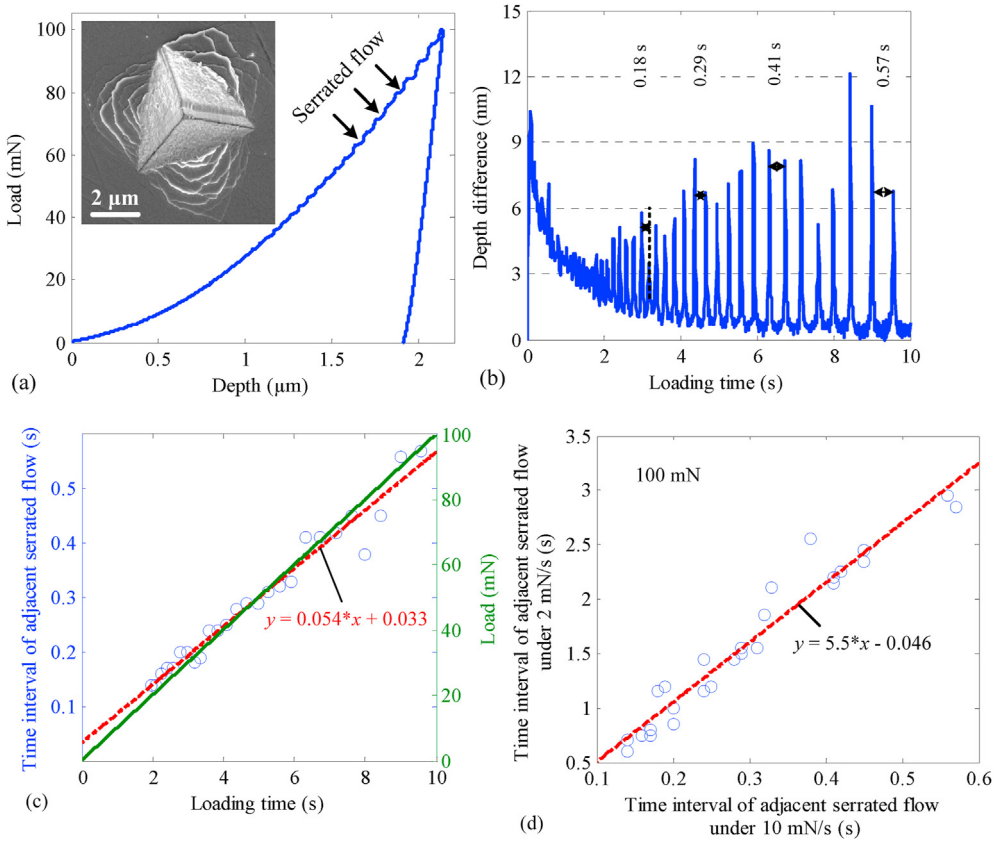

Fig. 2. Results obtained under the loading rate of 10 mN/s. (a) shows the load-depth curve and the corresponding morphology of residual indent. (b) The depth difference varies with the loading time. (c) Time interval of adjacent serrated flow as well as load varies with the loading time. (d) The correlation of the time interval of adjacent serrated flow obtained under 2 mN/s and 10 mN/s.

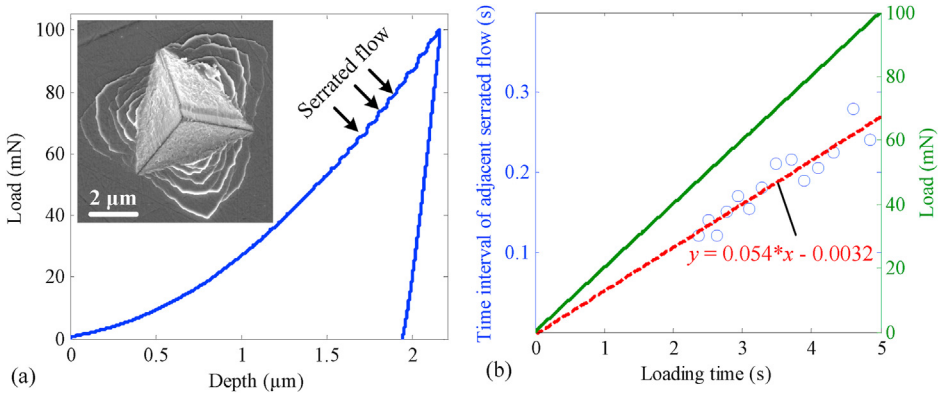

Fig. 3. Results obtained under the loading rate of 20 mN/s. (a) shows the load-depth curve and the corresponding morphology of residual indent. (b) Time interval of adjacent serrated flow as well as load varies with the loading time.

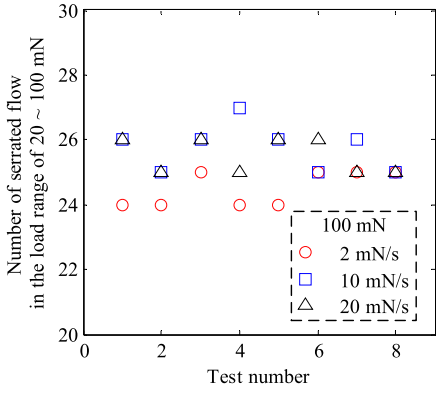

Fig. 4. Statistical results of the number of serrated flow in the load range of 20~100 mN under various loading rate.

From our current results, the previous understanding can be corrected that for the as-cast MG, the shear bands and the number of serrated flows are nearly independent of the used loading rate but high loading rate weakens the size of serrated flow (i.e. the height of peaks in the depth difference-loading time curve). Accordingly, our results strongly support the shear-band propagation dynamics (SBPD) model, and the shear-band nucleation dynamics (SBND) model may be not applicable.

Plastic deformation of MGs are determined by the applied stress. Shear banding is regarded as the main plastic deformation mechanism of MGs [14,15], and thus, shear banding event should also mainly depends on the applied stress. This can be strongly supported by these two facts related to the number of serrated flow and the shear band features around the residual indents obtained under various loading rates. When the stress applied by the cube-corner indenter reaches the critical value, shear banding event is triggered. Correspondingly, the shear band is gradually generated around and below the indent, and at the same time, serrated flow appears in the load-depth curve. After one shear banding event, the applied stress is released, and thus, further increase in the indentation load is required to reach the critical stress that triggers the next shear banding event. This may be the reason why shear bands and serrated flows are intermittent.

With regard to the effect of loading rate on the size of serrated flow (i.e. the height of peaks in the depth difference-loading time curve), it could be well explained by the SBPD model [25]. For relatively small loading rate, the propagation velocity of shear band is larger than the applied strain rate, and thus, the shear band could propagate adequately, resulting in relatively large serrated flow. Whereas, for relatively high loading rate, the applied strain rate overwhelms the propagation velocity of shear band. Prior to adequate propagation of the current shear band, the critical stress for triggering the next shear band is reached. Therefore, the current shear band is arrested, resulting relatively small serrated flow.

With regard to the phenomenon that the time interval of adjacent serrated flow increases with increase in the load as shown in Figs. 1(d), 2(c) and 3(b), it may be due to the following two reasons. Firstly, previous studies [42,43] indicate that the average contact pressure during loading process of nanoindentation tends to gradually decrease with increase in the indentation load. Although the stress that triggers shear banding event may be not the same of average contact pressure, they should be positive correlation. Thus, larger load increment is required to reach the same critical stress when the indentation load is high. On the other hand, shear band is considered to be formed by evolution of the so-called shear-transformation zone (STZs) [44]. For the high indentation load, more STZs should have been generated below the indenter, and thus, to trigger the evolution of large amounts of STZs, larger stress should be accumulated, requiring larger load increment, i.e., the increased time interval.

4. Conclusion

In summary, for further understanding the serrated flow and shear band behavior, a cube-corner indenter was employed to conduct nanoindentation tests on a Zr-based MG. By comparative experiments and analysis under various loading rates, it was seen that the shear bands and the number of serrated flows were nearly independent of the used loading rate but the size of serrated flow was greatly weakened under high loading rate. These results strongly support the shear-band propagation dynamics model, which are meaningful for achieving a general model that understands the effects of loading rate on the plastic deformation of MGs.

CRediT authorship contribution statement

Hu Huang: Conceptualization, Data curation, Investigation, Methodology, Writing - original draft, Writing - review & editing. **Minqiang Jiang:** Investigation, Supervision, Writing - review & editing. **Jiwang Yan:** Methodology, Supervision, Funding acquisition, Writing - review & editing.

Declaration of competing interest

The authors declare that they have no known competing financial interests or personal relationships that could have appeared to influence the work reported in this paper.

Acknowledgement

This work was supported by the National Natural Science Foundation of China (Grant No. 51705197), Science and Technology Project from the Education Department of Jilin Province (Grant No. JJKH20190014KJ), and Young Elite Scientists Sponsorship Program by CAST(YESS) (Grant No. 2017QNRC001).

References

[1] J. Pan, Y.P. Ivanov, W.H. Zhou, Y. Li, A.L. Greer, Strain-hardening and suppression of shear-banding in rejuvenated bulk metallic glass, Nature 578 (2020) 559–562.
[2] J. Plummer, W.L. Johnson, Is metallic glass poised to come of age? Nat. Mater. 14 (2015) 553–555.
[3] E. Ma, Tuning order in disorder, Nat. Mater. 14 (2015) 547–552.
[4] Y.H. Liu, G. Wang, R.J. Wang, D.Q. Zhao, M.X. Pan, W.H. Wang, Super plastic bulk metallic glasses at room temperature, Science 315 (2007) 1385–1388.
[5] T.Y. Chen, J.J. Li, S.H. Chen, C. Li, Shear band multiplication induced strong strain delocalization and high tensile ductility in amorphous thin films by metallic substrates, Int. J. Solid Struct. 195 (2020) 1–12.
[6] S.Y. Di, Q.Q. Wang, J. Zhou, Y.Y. Shen, J.Q. Li, M.Y. Zhu, K.B. Yin, Q.S. Zeng, L.T. Sun, B.L. Shen, Enhancement of plasticity for FeCoBSiNb bulk metallic glass with superhigh strength through cryogenic thermal cycling, Scripta Mater. 187 (2020) 13–18.
[7] Y. Du, W.C. Han, Q. Zhou, Y.H. Xu, H.M. Zhai, V. Bhardwaj, H.F. Wang, Enhancing the plasticity of a Ti-based bulk metallic glass composite by cryogenic cycling treatments, J. Alloys Compd. 835 (2020), 155247.
[8] F.A. Davani, S. Hilke, H. Rosner, D. Geissler, A. Gebert, G. Wilde, On the shear-affected zone of shear bands in bulk metallic glasses, J. Alloys Compd. 837 (2020), 155494.
[9] R. Hubek, M. Seleznev, I. Binkowski, M. Peterlechner, S.V. Divinski, G. Wilde, Intrinsic heterogeneity of shear banding: hints from diffusion and relaxation measurements of Co micro-alloyed PdNiP-based glass, J. Appl. Phys. 127 (2020), 115109.
[10] G.N. Yang, Y. Shao, C.T. Liu, K.F. Yao, How does the structural inhomogeneity influence the shear band behaviours of metallic glasses, Philos. Mag. A 100 (2020) 1663–1681.
[11] D. Sopu, S. Scudino, X.L. Bian, C. Gammer, J. Eckert, Atomic-scale origin of shear band multiplication in heterogeneous metallic glasses, Scripta Mater. 178 (2020) 57–61.
[12] S. Kuchemann, C.Y. Liu, E.M. Dufresne, J. Shin, R. Maass, Shear banding leads to accelerated aging dynamics in a metallic glass, Phys. Rev. B 97 (2018), 014204.
[13] Y. Du, Q. Zhou, Q. Jia, Y.D. Shi, H.F. Wang, J. Wang, Imparities of shear avalanches dynamic evolution in a metallic glass, Mater. Res. Lett. 8 (2020) 357–363.
[14] D.P. Wang, B.A. Sun, X.R. Niu, Y. Yang, W.H. Wang, C.T. Liu, Mutual interaction of shear bands in metallic glasses, Intermetallics 85 (2017) 48–53.
[15] A.L. Greer, Y.Q. Cheng, E. Ma, Shear bands in metallic glasses, Mater. Sci. Eng. R 74 (2013) 71–132.
[16] R. Maass, J.F. Loffler, Shear-band dynamics in metallic glasses, Adv. Funct. Mater. 25 (2015) 2353–2368.
[17] C.A. Schuh, T.C. Hufnagel, U. Ramamurty, Overview No.144 - mechanical behavior of amorphous alloys, Acta Mater. 55 (2007) 4067–4109.
[18] C.A. Schuh, T.G. Nieh, A nanoindentation study of serrated flow in bulk metallic glasses, Acta Mater. 51 (2003) 87–99.
[19] T. Burgess, K.J. Laws, M. Ferry, Effect of loading rate on the serrated flow of a bulk metallic glass during nanoindentation, Acta Mater. 56 (2008) 4829–4835.
[20] F.H. Dalla Torre, D. Klaumunzer, R. Maass, J.F. Loffler, Stick-slip behavior of serrated flow during inhomogeneous deformation of bulk metallic glasses, Acta Mater. 58 (2010) 3742–3750.
[21] B.A. Sun, S. Pauly, J. Tan, M. Stoica, W.H. Wang, U. Kuhn, J. Eckert, Serrated flow and stick-slip deformation dynamics in the presence of shear-band interactions for a Zr-based metallic glass, Acta Mater. 60 (2012) 4160–4171.
[22] X. Xie, Y.C. Lo, Y. Tong, J.W. Qiao, G.Y. Wang, S. Ogata, H.R. Qi, K.A. Dahmen, Y.F. Gao, P.K. Liaw, Origin of serrated flow in bulk metallic glasses, J. Mech. Phys. Solid. 124 (2019) 634–642.
[23] Y. Du, Q. Zhou, Y. Ren, W.W. Kuang, W.C. Han, S. Zhang, H.M. Zhai, H.F. Wang, Tailoring shear banding behaviors in high entropy bulk metallic glass by minor Sn addition: a nanoindentation study, J. Alloys Compd. 762 (2018) 422–430.
[24] B.A. Sun, S. Pauly, J. Hu, W.H. Wang, U. Kuhn, J. Eckert, Origin of intermittent plastic flow and instability of shear band sliding in bulk metallic glasses, Phys. Rev. Lett. 110 (2013) 225501.
[25] R. Maass, D. Klaumunzer, J.F. Loffler, Propagation dynamics of individual shear bands during inhomogeneous flow in a Zr-based bulk metallic glass, Acta Mater. 59 (2011) 3205–3213.
[26] W. Zheng, Y.J. Huang, G.Y. Wang, P.K. Liaw, J. Shen, Influence of strain rate on compressive deformation behavior of a Zr-Cu-Ni-Al bulk metallic glass at room temperature, Metallurgical and Materials Transactions a-Physical Metallurgy and Materials Science 42A (2011) 1491–1498.
[27] S. Gonzalez, G.Q. Xie, D.V. Louzguine-Luzgin, J.H. Perepezko, A. Inoue, Deformation and strain rate sensitivity of a Zr-Cu-Fe-Al metallic glass, Mater. Sci. Eng., A 528 (2011) 3506–3512.
[28] W.F. Ma, H.C. Kou, J.S. Li, H. Chang, L. Zhou, Effect of strain rate on compressive behavior of Ti-based bulk metallic glass at room temperature, J. Alloys Compd. 472 (2009) 214–218.
[29] F.H. Dalla Torre, A. Dubach, A. Nelson, J.F. Loffler, Temperature, strain and strain rate dependence of serrated flow in bulk metallic glasses, Mater. Trans. 48 (2007) 1774–1780.
[30] T.G. Nieh, C. Schuh, J. Wadsworth, Y. Li, Strain rate-dependent deformation in bulk metallic glasses, Intermetallics 10 (2002) 1177–1182.
[31] C.A. Schuh, T.G. Nieh, Y. Kawamura, Rate dependence of serrated flow during nanoindentation of a bulk metallic glass, J. Mater. Res. 17 (2002) 1651–1654.
[32] Q. Zhou, Y. Du, W.C. Han, Y. Ren, H.M. Zhai, H.F. Wang, Identifying the origin of strain rate sensitivity in a high entropy bulk metallic glass, Scripta Mater. 164 (2019) 121–125.
[33] C.A. Schuh, A.C. Lund, T.G. Nieh, New regime of homogeneous flow in the deformation map of metallic glasses: elevated temperature nanoindentation experiments and mechanistic modeling, Acta Mater. 52 (2004) 5879–5891.
[34] H. Huang, J.L. Zhang, C.H. Shek, J.W. Yan, Effects of pre-compression deformation on nanoindentation response of Zr65Cu15Al10Ni10 bulk metallic glass, J. Alloys Compd. 674 (2016) 223–228.
[35] H. Huang, M.Q. Jiang, J.W. Yan, Softening of Zr-based metallic glass induced by nanosecond pulsed laser irradiation, J. Alloys Compd. 754 (2018) 215–221.
[36] A.C. Fischer-Cripps, Nanoindentation, Springer, New York, 2011.
[37] H. Huang, H. Zhao, Indenter geometry affecting indentation behaviors of the Zr-based bulk metallic glass, Mater. Trans. 55 (2014) 1400–1404.
[38] H. Huang, J.W. Yan, On the surface characteristics of a Zr-based bulk metallic glass processed by microelectrical discharge machining, Appl. Surf. Sci. 355 (2015) 1306–1315.
[39] H. Huang, J.W. Yan, Microstructural changes of Zr-based metallic glass during microelectrical discharge machining and grinding by a sintered diamond tool, J. Alloys Compd. 688 (2016) 14–21.
[40] H. Huang, H.W. Zhao, Z.Y. Zhang, Z.J. Yang, Z.C. Ma, Influences of sample preparation on nanoindentation behavior of a Zr-based bulk metallic glass, Materials 5 (2012) 1033–1039.
[41] W.H. Jiang, M. Atzmon, Rate dependence of serrated flow in a metallic glass, J. Mater. Res. 18 (2003) 755–757.
[42] T. Juliano, Y. Gogotsi, V. Domnich, Effect of indentation unloading conditions on phase transformation induced events in silicon, J. Mater. Res. 18 (2003) 1192–1201.
[43] H. Huang, J.W. Yan, On the mechanism of secondary pop-out in cyclic nanoindentation of single-crystal silicon, J. Mater. Res. 30 (2015) 1861–1868.
[44] M.L. Falk, J.S. Langer, Dynamics of viscoplastic deformation in amorphous solids, Phys. Rev. E 57 (1998) 7192–7205.